



The Effect of Hydrothermal Aging on the Low-Velocity Impact Behavior of Multi-Walled Carbon Nanotubes Reinforced Carbon Fiber/Epoxy Composite Pipes

Memduh Kara¹ · Safa Ak² · Mesut Uyaner³ · Alper Gunoz¹ · Yusuf Kepir¹

Received: 16 October 2020 / Accepted: 5 June 2021 / Published online: 8 July 2021
© The Author(s), under exclusive licence to Springer Nature B.V. 2021

Abstract

Chemical transmission lines, petroleum and natural gas lines, pressure vessels, and pipes used in thermal facilities are expected to maintain their mechanical properties for many years without being damaged and not to be corroded in working conditions. The composite materials are the right candidate for these harsh conditions due to their superior properties. Reinforcement of nanoadditives to composite materials improves both the mechanical properties and the resistance to environmental conditions, thereby increasing the lifetime. In this study, multi-walled carbon nanotube (MWCNT) reinforced [$\pm 55^\circ$] carbon fiber/epoxy composite pipes produced with filament wound method were used. It was hydrothermally aged in 80 °C distilled water for 1, 2, 3 weeks in order to examine the effect of environmental conditions. In order to investigate its resistance against loads that may occur in working conditions, ring tensile tests (ASTM D 2290–16 procedure A), and low-velocity impact tests at 5, 10, 15 J, energy levels were carried out. The effect of hydrothermal aging on neat and MWCNT added epoxy composite had been examined by considering the aging period. Consequently, the impact resistance of neat and MWCNT added samples decreased with the aging process. Besides, tangential tensile strength loss was 17% in MWCNT reinforced sample and 13% in the neat sample.

Keywords Carbon-reinforced epoxy · Low-velocity impact · MWCNT · Hydrothermal aging

1 Introduction

Fiber-reinforced plastics (FRPs) produced by the filament wound method have been widely used for underground transportation of fluid materials such as drinking water, wastewater, thermal water, oil, and natural gas [1–5]. Filament wound FRPs have many potential

✉ Memduh Kara
memduhkara@mersin.edu.tr

¹ Mersin University, Dept. of Mechanical Engineering, Engineering Faculty, Yenişehir, Mersin, Turkey

² Institute of Science and Technology, Necmettin Erbakan University, Dept. of Mechanical Engineering, Konya, Turkey

³ Faculty of Aeronautics and Astronautics, Dept. of Aeronautical Engineering, Necmettin Erbakan University, Konya, Turkey

advantages over metal pipes, such as good corrosion resistance, high specific strength, and thermal insulation [6–9]. Despite their superior physical and chemical properties, FRPs can be damaged due to the loads and stresses they are exposed to in working conditions. Damage to the composite material significantly reduces the strength of the entire installation. Therefore, it is crucial to increase the resistance of composite materials against various loadings. Nowadays, nanoadditives are added to the resins of composite materials, so the bond between the resin and the fiber is strengthened, and the material's resistance to external loads is increased [10]. Recent studies have shown that the addition of nanoadditives to the resin significantly improves explosion strength [11], tangential tensile strength [11–13], and contact force [14–16] in composite materials. Kara et al. [14] in their study, applied low speed impact test to carbon fiber/epoxy composite pipes reinforced with MWCNT. As a result of the study, they observed that MWCNT reinforcement to carbon fiber/epoxy composite pipes increased the rigidity and strength of the samples. Fan et al. [17] provided the strengthening of the interfacial strength of glass fiber reinforced composite materials by adding inorganic nanofillers.

Materials are hydrothermally aged in order to investigate the resistance of composite materials exposed to various environmental effects under working conditions. The effects of aging on the mechanical strength of composite materials can be determined by mechanical tests performed before and after aging [18, 19]. Besides, nanoadditives are added to composite materials to reduce the adverse effects of aging on composite materials. There are some studies on this subject in the literature [20–22]. Nayak et al. [20] investigated the addition of nano TiO_2 filler on residual flexural strength of hydrothermally aged glass fiber reinforced polymer composites. The results showed that the addition of 0.1 wt.% TiO_2 improved residual flexural strength by approximately 19%, reduced moisture diffusion coefficient by about 9%.

When filament wound composite pipes are subjected to low-velocity impact such as dropping of tools under the working conditions invisible damage consisting of internal delamination in pipes could occur. In order to prevent problems that may occur in such a situation, it is essential to investigate the impact response of the material and ways to increase its impact resistance. There are studies [23–27] in the literature showing that low-velocity impact resistance of composite materials is increased with nanoadditives. Taraghi and Fereidoon [28] performed low velocity impact tests at six different energy levels on MWCNT reinforced plates in their study. As a result of the study, they observed that the energy absorption capacity of the samples with 0.5 wt.% MWCNT was increased by 16% compared to the neat samples. Ranjbar and Feli [29] investigated the low velocity impact response of glass/epoxy composite beams reinforced with various weight percentages of MWCNTs in their study. As a result of the study, they observed that the displacement decreased and the rigidity increased in the MWCNT reinforced samples compared to the neat samples.

It is quite essential to observe the damage behavior of filament wound composite pipes subjected to external mechanical loads. Hoop tensile test is applied to determine tangential tensile strength and damage behavior of filament wound composite pipes. There are studies [30–32] in the literature in which hoop tensile testing is applied to determine the tangential tensile strength of filament wound composite pipes. Sepetcioglu et al. [33] performed a hoop tensile test on 0.25 wt.% graphene nanoplatelets (GnP) reinforced filament winding basalt fiber/epoxy composite (BFRP) samples. As a result of the study, they observed that the nano additive increased the hoop tensile strength of the samples by approximately 5%. Üstün et al. [11] conducted a hoop tensile test on MWCNT reinforced carbon/epoxy composite pipes in their study. As a result of the study, they observed that the tangential tensile strength of the MWCNT added samples was 26.2% higher than the neat samples.

In this study, carbon fiber reinforced polymer (CFRP) composite pipes with 0.3 wt.% MWCNT and neat samples were hydrothermally aged and then subjected to hoop tensile and low-velocity impact tests. The effect of hydrothermal aging on mechanical properties of filament winding composite pipes and the role of nanoadditives in eliminating these adverse effects were investigated.

2 Material and Methods

The hydrothermal aging process was performed in a distilled water environment at a temperature of 80 °C for 1, 2, 3 weeks for a neat matrix and 0.3 wt.% of MWCNT reinforced CFRPs in a matrix structure. In some studies in the literature [34–36], it was stated that the best mechanical properties would be obtained by adding 0.3 wt.% MWCNT to the epoxy matrix. In light of this information, 0.3 wt.% of MWCNT was added to the matrix in this study. In order to measure the effect of the aging process on tangential stresses of the pipes, hoop tensile strength test was carried out according to ASTM D 2290 Procedure A [37]. Besides, low-velocity impact test was performed at 5, 10, 15 J energy levels in order to determine the effect of hydrothermal aging on the impact resistance of the pipes.

Damage and deformation mechanisms occurring in the impacted sample were visualized with an optical microscope, the damage mechanisms formed were grouped, and their effects on the composite material were explained.

2.1 Production of Composite Pipes

Neat and 0.3 wt.% MWCNT reinforced, filament wound carbon fiber nanocomposite pipes were used in this study. Each pipe was produced in accordance with the ring tensile testing device with an inside diameter of 72 mm and a length of 300 mm.

In this study, Araldite MY 740, the Bisphenol-A epoxy resin type, was used as the matrix, Aradur HY 918 anhydride hardener was used as the hardener, and DY 062 was used as the accelerator. The matrix materials used were purchased from Huntsman. In the production of pipes, A-42 12 K continuous carbon fiber was used purchased from DowAksa. In order to reinforce the epoxy matrix, MWCNT reinforcement was purchased from Nanocly. The mechanical properties of the matrix, fiber, and MWCNT are given in Table 1.

Figure 1 shows the process of reinforcing epoxy with MWCNT. Primarily MWCNTs are prepared to the desired weight ratio were added to epoxy resin (I). In order to achieve a homogeneous mixture, MWCNTs were mixed with a mechanical stirrer for 30 min (II) and an ultrasonic probe sonicator (III) for 10 min. The temperature of the mixture was kept under control by a thermometer, while ultrasonic mixing was performed. The air bubbles formed in the mixture were removed by vacuum degassing (IV) at the end of the ultrasonic mixing process. Then the hardener was added to the epoxy resin (V) and mixed once more with the mechanical stirrer (VI). As soon as the MWCNT reinforced epoxy resin had been prepared, the filament wound processing was immediately realized with a $\pm 55^\circ$ winding angle (see Fig. 2). After the filament wound process was accomplished, on the recommendation of the manufacturer, the curing process was implemented firstly at 180 °C for 2 h and then at 120 °C for 12 h. Figure 3 presents the dimensions of the specimens used in the experiments.

Table 1 Properties of resin, fiber, and MWCNT used in the production of CFRPs [38]

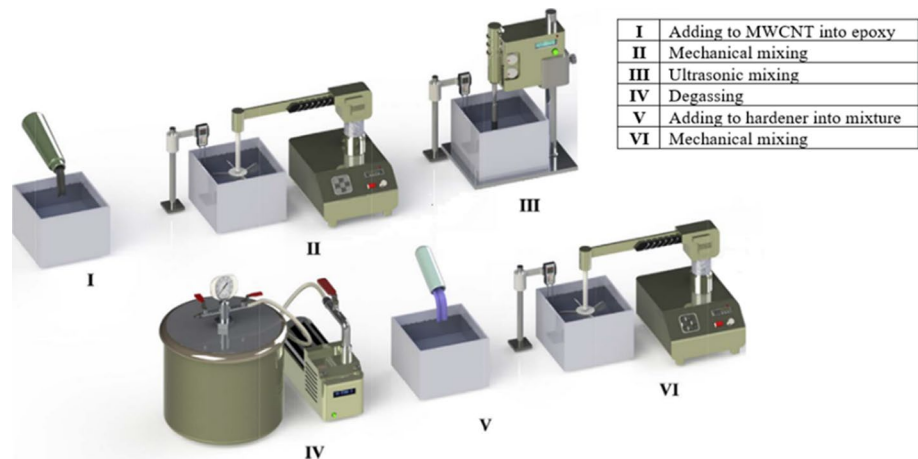
Material	Elasticity Modulus (E, GPa)	Tensile Strength (σ , GPa)	Elongation at Break (%)	Density (ρ , g/cm ³)
Epoxy Resin	3.2–3.8	0.075–0.080	3–4	1.25
Carbon Fiber	-	4.2	1.8	1.8
MWCNT	1000	10–60	10	1.3–2

2.2 The Hydrothermal Aging

In order to carry out the hydrothermal aging process at distilled water, an aging unit with a volume of 64 L made of 5 mm thick glass was used (see Fig. 4). The aging temperature was selected as 80 °C, which is close to the glass transition temperature of epoxy resin and used in hydrothermal aging of epoxy resin composites in literature [39]. Hydrothermal aging was performed on neat, and MWCNT reinforced CFRPs for 1, 2, and 3 weeks.

2.3 Hoop Tensile Strength Test

Hoop tensile strength test was implemented following ASTM D 2290 Procedure A [37]. Test specimens were prepared from eight layered CFRPs under the Ref. [37] (see Fig. 5). Test specimens were prepared according to the ASTM D 2290 Procedure A [37]. According to Procedure A [37], specimens shall have a minimum overall width of 22.86 mm, a minimum width in the reduced sections of 13.97 mm, and notching on both sides of the sample was left to the user's choice. In the hoop tensile test, conditions such as tensile speed, humidity, and temperature and specimen thickness of the test machine jaw were taken into consideration. The standard laboratory ambient temperature is

**Fig. 1** The process of reinforcing MWCNT into epoxy [14]

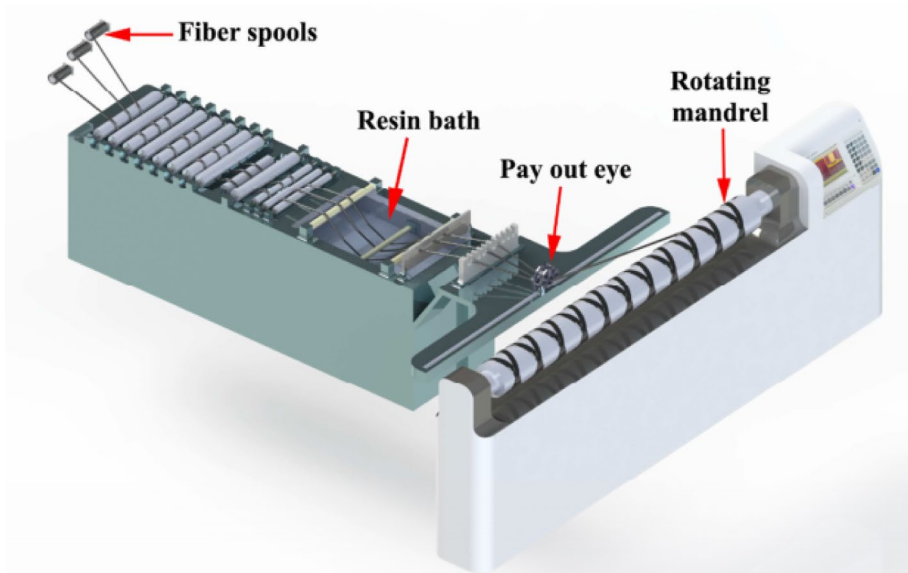


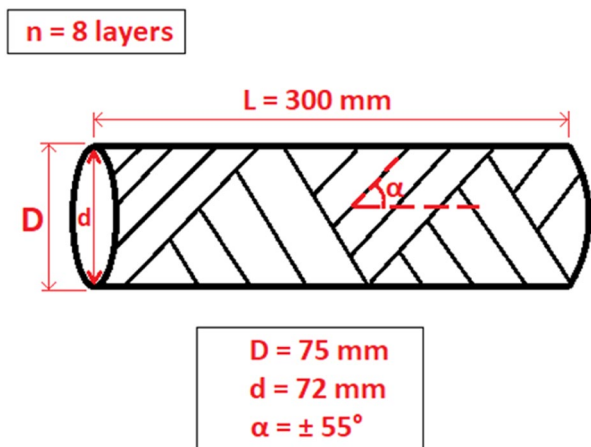
Fig. 2 Filament winding process [14]

23 ± 2 °C, humidity, 55 ± 5%. The test speed is at least 2.54 mm/min. The hoop tensile test rig is shown in Fig. 6.

In this test, the strength values of the composite pipe specimen could be determined by Eq. 1. In the equation, σ_T , P_b , A_m denote the hoop tensile strength value (MPa) of the specimen, the maximum load value (N), and the minimum cross-sectional area (mm²), respectively.

$$\sigma_T = \frac{P_b}{2A_m} \tag{1}$$

Fig. 3 CFRP in configurations $[\pm 55^\circ]_4$ produced by the filament winding method



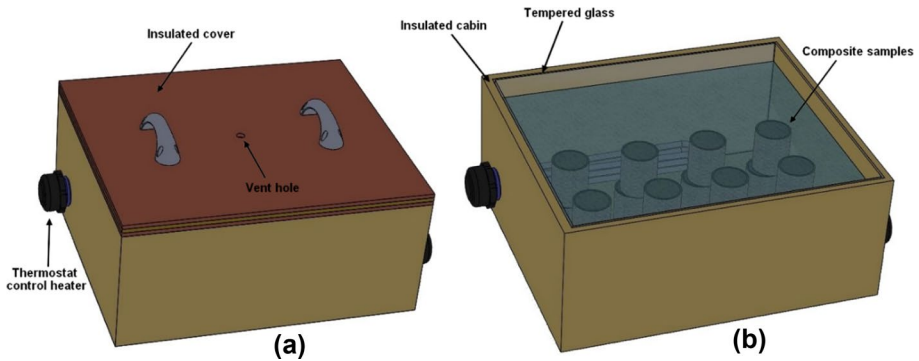


Fig. 4 Schematic representation of the hydrothermal aging unit (a) with and (b) without a layered insulation panel cover

2.4 Low-Velocity Impact Test

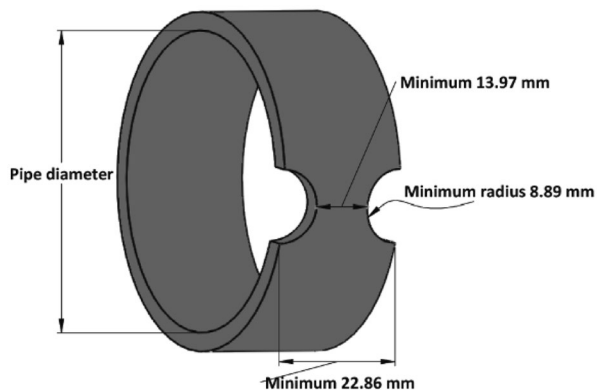
The low-velocity impact experiments were performed on the neat and MWCNT reinforced CFRPs for various energy levels as 5, 10, 15 J. The corresponding impact velocities to these energies, are 1.255, 1.775, 2.174 m/s, respectively. The impactor has a mass of 6.35 kg and a semi-spherical geometry of diameter 24 mm. Composite pipes were exposed to low-velocity impact tests with the device shown in Fig. 7. PCB Quartz ICP Force Sensor (M202B04) is used as the force sensor between the tup and the mass of the impactor. The kinematic analysis was carried out via in-house developed codes [40].

3 Results and Discussion

3.1 Hoop Tensile Strength Test Results

Hoop tensile strength test carried on until specimens were broken. Experiments were repeated three times for each case, and the average values were determined. Figure 8 show the relationship between the applied load and the displacement for neat and MWCNT

Fig. 5 Reduced section specimen following Procedure A [37]



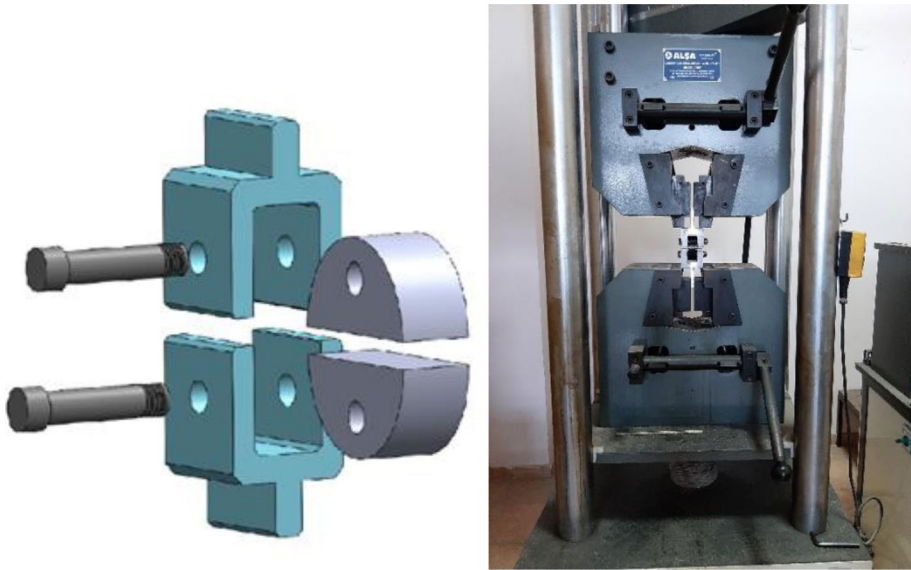
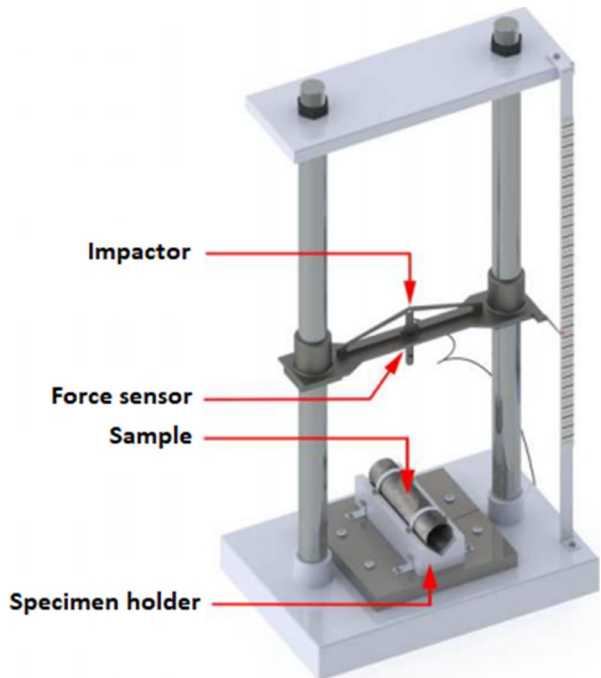


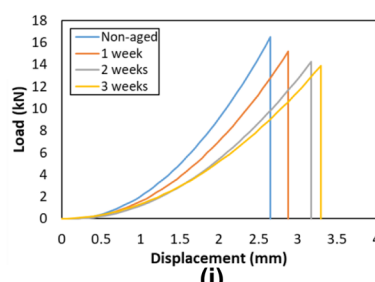
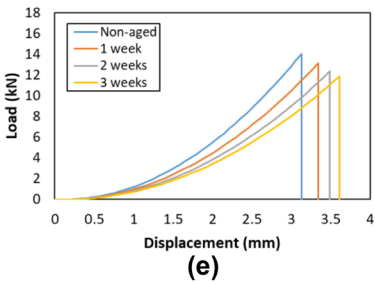
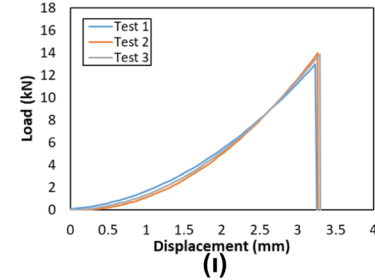
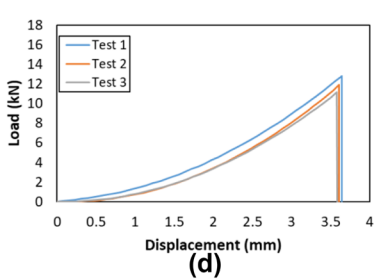
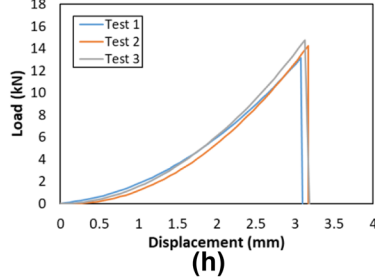
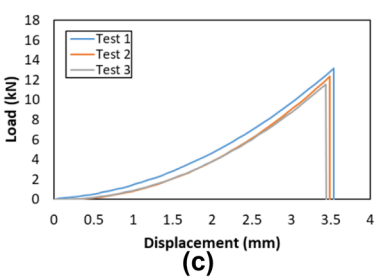
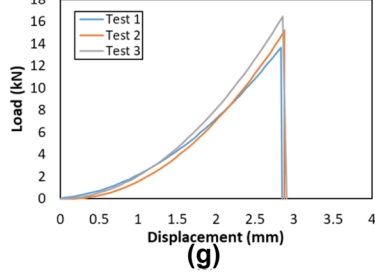
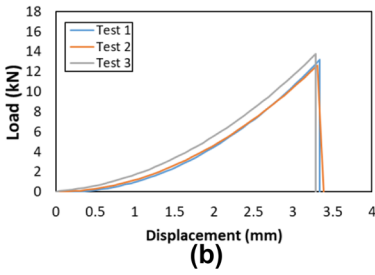
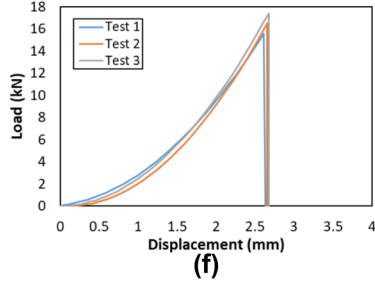
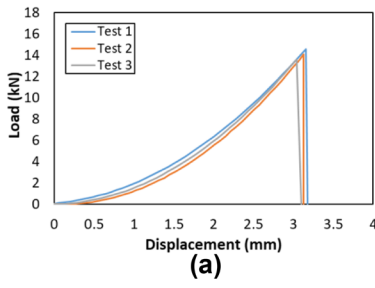
Fig. 6 Hoop tensile test instrument

reinforced samples tested at the different aging times. These curves show good reproducibility for different cases. Experimental results were regrouped in Table 2.

The damage to the eight layered CFRPs unexposed to and exposed to hydrothermal aging for different time intervals as a result of the hoop tensile test were shown in Fig. 9.

Fig. 7 Low-velocity test instrument [14]





◀**Fig. 8** Load–displacement curves for (a) Non-aged CFRP; (b) 1 week, (c) 2 weeks, (d) 3 weeks aged CFRPs, and (e) representative of CFRPs, (f) non-aged MWCNT reinforced CFRP; (g) 1 week, (h) 2 weeks, (i) 3 weeks aged MWCNT reinforced CFRPs, (i) representative of MWCNT reinforced CFRPs

When the hoop tensile strength value was reached in both samples, it was observed fiber rupture and splitting from the notch region in the direction of the winding angle of $\pm 55^\circ$.

When the images of the samples are examined, it is seen that the resin flow is more evident in some samples after three weeks. This situation is due to the transition of nanoparticles to the external environment through diffusion, and the porosity formed in the structure facilitates the flow of epoxy resin. Also, it may occur that the epoxy cannot be distributed homogeneously into the composite structure during manufacturing.

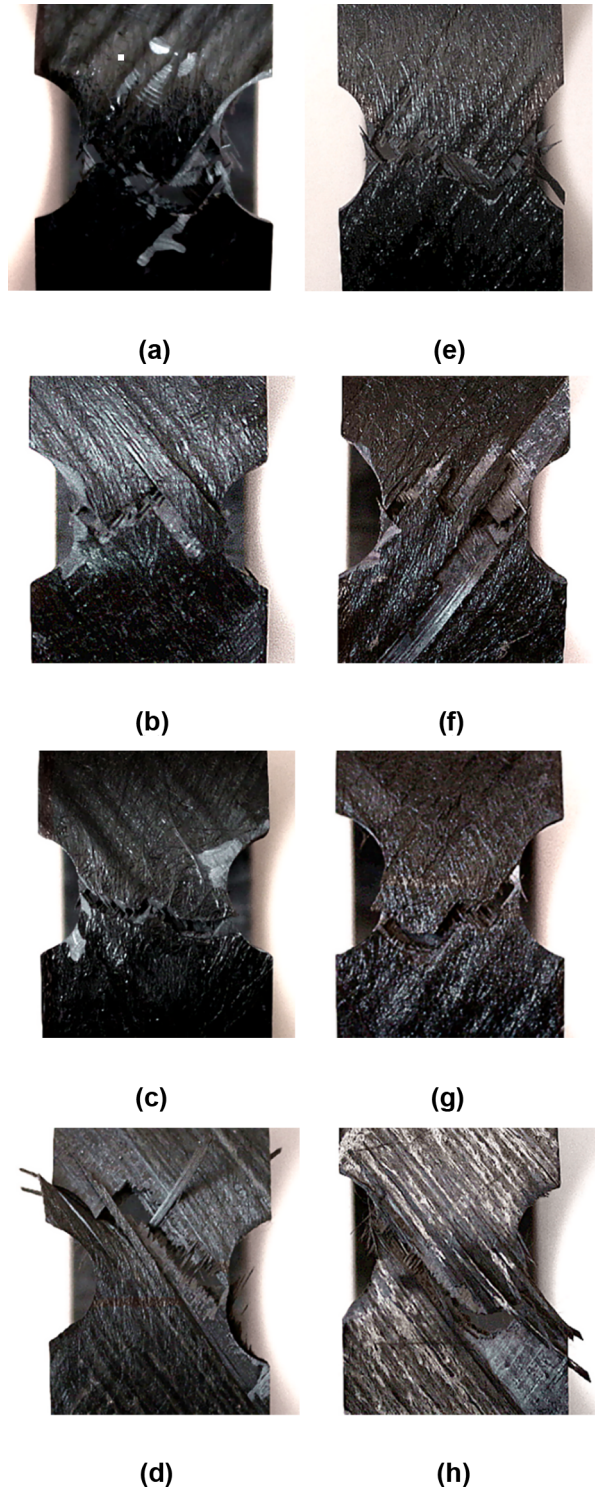
Figure 10 provides the average hoop tensile strength values of samples exposed to hydrothermal aging and unexposed to hydrothermal aging. The average hoop tensile strength values of non-aged CFRPs was found to be 402 MPa. After three weeks of aging of CFRPs, the tensile strength values were measured as an average 345 MPa with a 14% decrease compared to the tensile strength values of the non-aged CFRPs.

The average hoop tensile strength values of non-aged MWCNT reinforced CFRPs was 471 MPa. As a result of measurements after three weeks of aging of MWCNT reinforced CFRPs, the tensile strength values were measured as an average 389 MPa with a 17% decrease compared to the tensile strength values of the non-aged MWCNT reinforced CFRPs.

Table 2 Mechanical properties of composite pipes exposed to hydrothermal aging

Aging time (weeks)	Tests	Neat samples		MWCNT reinforced samples	
		Max load (kN)	Displacement at break (mm)	Max load (kN)	Displacement at break (mm)
0	1	14.564	3.180	15.561	2.638
	2	14.079	3.127	16.479	2.647
	3	13.565	3.098	17.400	2.668
	Average	14.069	3.135	16.480	2.651
	Standard Deviation	0.500	0.042	0.920	0.015
1	1	13.201	3.345	13.662	2.851
	2	12.567	3.390	15.193	2.879
	3	13.745	3.287	16.424	2.909
	Average	13.171	3.341	15.093	2.880
	Standard Deviation	0.590	0.052	1.384	0.029
2	1	13.170	3.544	13.149	3.099
	2	12.360	3.476	14.252	3.167
	3	11.580	3.444	14.755	3.185
	Average	12.370	3.488	14.052	3.150
	Standard Deviation	0.795	0.051	0.821	0.045
3	1	12.795	3.643	12.983	3.252
	2	11.884	3.610	13.938	3.266
	3	11.139	3.584	13.869	3.298
	Average	11.939	3.612	13.597	3.272
	Standard Deviation	0.829	0.030	0.533	0.024

Fig. 9 Images of damage for (a) Non-aged CFRP; (b) 1 week, (c) 2 weeks, and (d) 3 weeks aged CFRPs, (e) non-aged MWCNT reinforced CFRP; (f) 1 week, (g) 2 weeks, and (h) 3 weeks aged MWCNT reinforced CFRPs



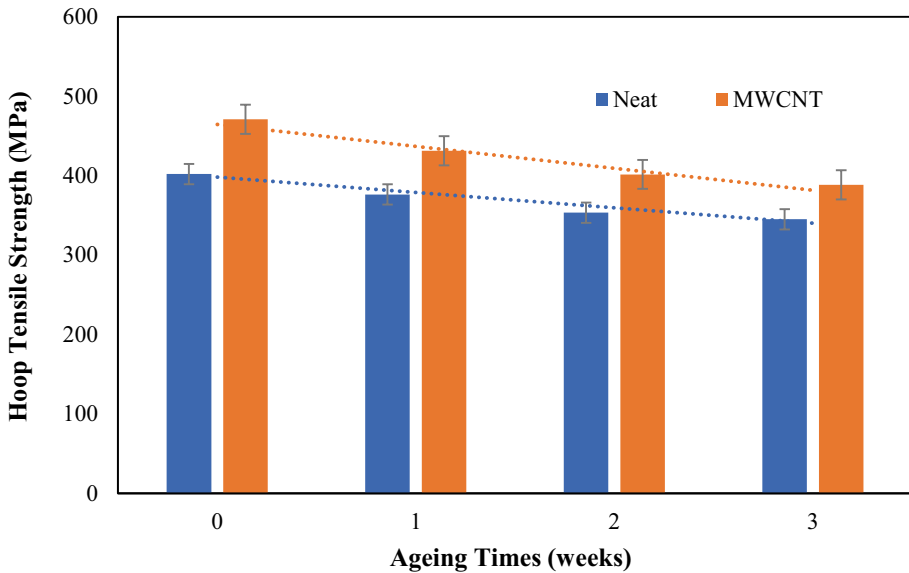


Fig. 10 Average hoop tensile strength of the CFRPs unexposed to and exposed to the hydrothermal aging process

Tangential strength values were higher in MWCNT reinforced pipes than non-reinforced pipes for all aging periods. As stated in the study of Taşyurek and Tarakcioğlu [12], the addition of MWCNT strengthens the fiber-matrix interface bonds. Based on a loading situation, the damage first observed in composite materials is generally the debonding of fiber-matrix interface [14, 33]. Strengthening the interfacial bonds with MWCNT reinforcement resulted in debonding damage of the fiber-matrix interface at higher strength values. Even if matrix rupture occurred, MWCNT could continue to serve as a bridge between the fibers without breaking. Therefore, it was observed that reinforced samples had higher strength values.

However, as the aging time increases, the strength reduction is higher in nanoparticle added samples. Depending on time and temperature, the epoxy flow causes deterioration of the mechanical bonds formed by the nanoparticles in the matrix structure and decreasing its functionality. In samples without nanoparticle reinforcement, epoxy flow causes some of the matrix cavities due to manufacturing to be eliminated and less loss of strength.

3.2 Low-Velocity Impact Test Results

Low-velocity impact test was performed at 5, 10, 15 J energy levels in neat epoxy and 0.3 wt.% MWCNT added composite pipes aged for 1, 2, 3 weeks in the hydrothermal aging unit. There are non-aged control samples in each pipe group. The low-speed impact test was repeated at least three times for each sample at all impact energy levels. With the data obtained from the experiments, force-time (F-t), and force-displacement (F-d) graphs were plotted and the effect of aging times and the addition of nanoparticles on impact resistance and impact damage in composite pipes were examined. The data obtained as a result of the experiments were presented in Table 3.

Table 3 The values obtained from the force histories

Aging Time (Weeks)	Impact Energy (J)	Neat samples			MWCNT reinforced samples		
		Maximum Contact Force (N)	Time (ms)	Displacement (mm)	Maximum Contact Force (N)	Time (ms)	Displacement (mm)
0	5	1430.60 ± 57.22	16.68 ± 0.67	5.50 ± 0.17	1840.85 ± 73.63	10.96 ± 0.44	3.94 ± 0.16
	10	1544.74 ± 92.54	19.20 ± 1.15	8.85 ± 0.44	2006.65 ± 105.52	14.30 ± 0.72	7.02 ± 0.42
	15	1627.43 ± 32.55	20.08 ± 0.40	10.90 ± 0.27	2181.25 ± 97.64	14.28 ± 0.64	8.66 ± 0.17
1	5	1361.04 ± 40.83	16.68 ± 0.52	5.50 ± 0.22	1724.80 ± 68.99	14.24 ± 0.43	4.68 ± 0.16
	10	1502.05 ± 90.12	18.16 ± 0.73	8.91 ± 0.26	1897.12 ± 75.88	17.90 ± 0.57	8.22 ± 0.21
	15	1495.50 ± 62.81	19.52 ± 0.82	11.32 ± 0.51	1998.22 ± 75.93	18.48 ± 0.48	10.69 ± 0.23
2	5	1296.31 ± 19.44	13.98 ± 0.17	5.52 ± 0.09	1640.75 ± 32.82	14.46 ± 0.25	4.92 ± 0.09
	10	1421.25 ± 63.96	16.26 ± 0.57	8.92 ± 0.27	1701.73 ± 68.07	17.32 ± 0.57	8.62 ± 0.31
	15	1491.70 ± 29.83	21.04 ± 0.81	11.65 ± 0.63	1914.44 ± 71.16	18.88 ± 0.42	10.76 ± 0.14
3	5	1248.47 ± 38.70	14.28 ± 0.46	5.58 ± 0.18	1364.86 ± 34.12	14.18 ± 0.49	5.29 ± 0.22
	10	1345.96 ± 40.38	15.04 ± 0.30	8.97 ± 0.22	1490.78 ± 38.76	17.06 ± 0.55	8.87 ± 0.18
	15	1375.93 ± 41.23	20.94 ± 0.44	12.13 ± 0.57	1752.62 ± 63.45	18.14 ± 0.41	10.88 ± 0.25

3.2.1 Force–Time Histories

Figures 11, 12, and 13 show force–time plots of samples with 5, 10, 15 J impact energy applied, non-aged, and aged for 1, 2, 3 weeks, respectively.

As the impact energy increases in all samples, the highest contact force value obtained from the experiments also increases. For all impact energy levels, higher contact force values were obtained in MWCNT added samples compared to the non-reinforced ones. With the increase of impact energy, the maximum contact force value increased more than the neat samples in MWCNT addition samples. Therefore, 0.3 wt.% MWCNT reinforcement dramatically contributes to the stiffness of the pipe. When the literature was examined, some studies presented similar results [14, 24, 29, 41]. In these studies, the stiffness of composite materials increased with the addition of different amounts of MWCNT. Moreover, Kara et al. [14] observed an increase in the stiffness of carbon fiber epoxy composite materials when they added 0.3 wt.% MWCNT to the same matrix (bisphenol-A epoxy resin).

It is observed that hydrothermal aging negatively affects the stiffness of the samples exposed to the impact. Because, depending on the aging time, the highest contact force obtained from the samples decreases.

The highest contact force in MWCNT reinforced samples was higher than neat samples. Significant decreases in maximum contact force occurred as the aging period was extended. These decreases in the highest contact force also show that the impact resistance decreases. The most significant decrease in the maximum contact force occurred in MWCNT reinforced samples and approximately 26% decrease occurred after three weeks of aging. This decrease can be caused by the diffusion of nanoparticles from resin to water and porosity in the matrix.

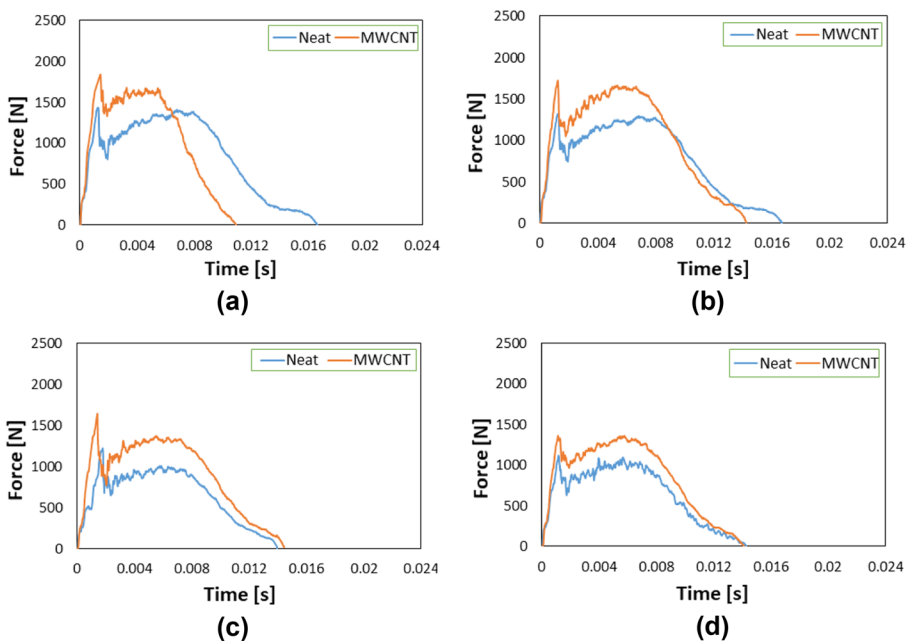


Fig. 11 Contact force histories at 5 J energy level for (a) Non-aged (b) 1 week, (c) 2 weeks, and (d) 3 weeks aged CFRPs

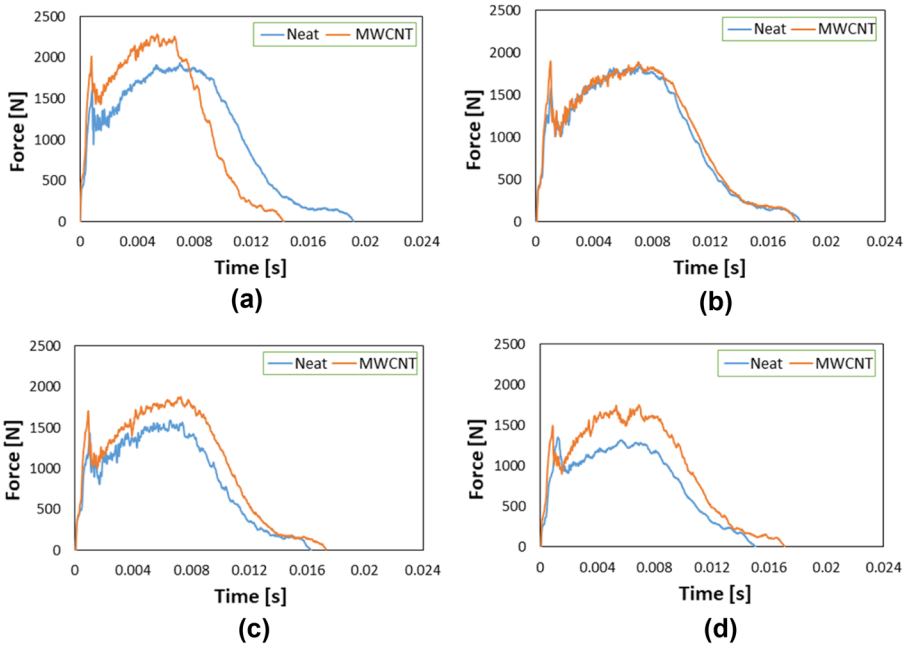


Fig. 12 Contact force histories at 10 J energy level for (a) Non-aged (b) 1 week, (c) 2 weeks, and (d) 3 weeks aged CFRPs

3.2.2 Force–Displacement Histories

Figures 14, 15, and 16 show force–displacement plots of 5, 10, and 15 J impact energy applied samples. Force–displacement curves occur in three different ways, depending on the rebound of the striker, the stub and the piercing of the specimen. In the experiments conducted in this study, the striker bounced back from the sample after the impact for all energy levels. The curves obtained are closed type curves. The maximum loading value that the specimens could withstand was not determined as there was no penetration in the samples [42].

In the force–displacement curve, the force drops when it reaches a specific value. This value is shown as “ F_1 ” in Fig. 14a. The F_1 force does not represent the onset of physical damage because non-critical matrix cracks and small delaminations during the impact may occur at lower force values. The F_1 force expresses the initial value of change in rigidity characteristic (ASTM D7136) [43]. For experiments at all impact energy levels, the value of F_1 was obtained higher in MWCNT reinforced composite samples. The addition of MWCNT to composite specimens increases rigidity. The oscillations in the loading phase of the force–displacement curve indicate the damages that occurred in the sample.

With the increasing impact energy level, the amount of deformation in all samples also increases. The addition of nanoparticles increased rigidity of the pipes, and accordingly, the maximum displacement value was seen in neat samples.

When the effects of aging and aging period are examined, the aging time of neat and MWCNT reinforced samples for all impact energy levels caused a decrease in F_1 force values. This decrease indicates a decrease in stiffness value. While the displacement values

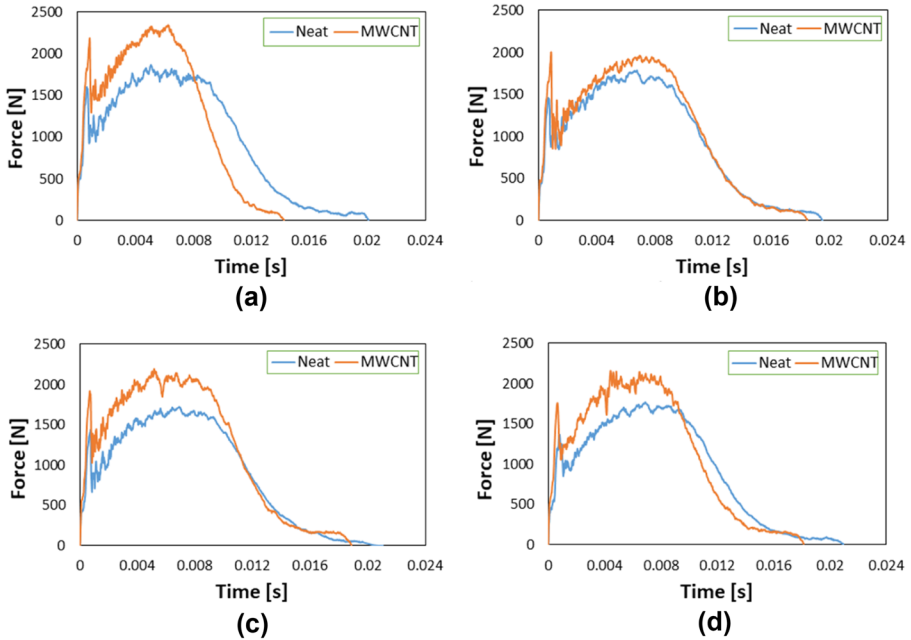


Fig. 13 Contact force histories at 15 J energy level for (a) Non-aged (b) 1 week, (c) 2 weeks, and (d) 3 weeks aged CFRPs

of MWCNT reinforced samples increased at all impact energy levels due to aging, the displacement values of 5 and 10 J impact energy levels of neat samples were nearly the same. They increased at 15 J impact energy levels.

3.3 Damage Mechanisms

The damages of the samples subjected at 5, 10, 15 J energy levels were examined with an optical microscope. The impacted samples were cut from the contact areas of the striker tip for examination. Subsequently, the damage mechanisms in the sections were displayed.

Damage formation in samples was observed at all impact energy levels. As expected, with increasing impact energy, the area of the damaged area increases, and the deformation mechanism is visible. Damage at all impact energy levels was mainly in the form of crack formation and delamination. At 10, 15 J energy levels, this damage occurred, and the number of damaged layers increased.

The addition of nanoparticles contributed to the homogeneous dissipation of impact energy in the material. In this way, nanoparticles prevented large deformations in the local area within the structure. As a result, delamination, which is the predominant damage mechanism in neat samples, has been replaced by matrix cracks that can be seen in all layers in nanoparticle-added samples. Thus, nanoparticle added samples absorbed more impact energy, and they are more resistant against impacts. Figure 17 gives cross-sectional images of non-reinforced and nanoparticle reinforced samples that have not been subjected to the aging process, damaged at different energy levels.

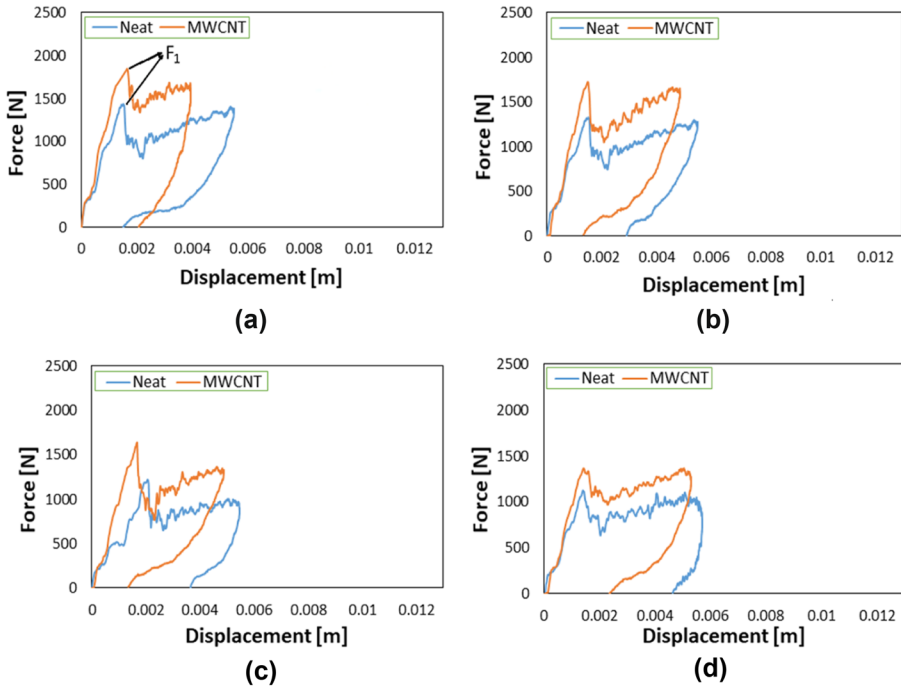


Fig. 14 Contact force–displacement variations at 5 J energy level for (a) Non-aged (b) 1 week, (c) 2 weeks, and (d) 3 weeks aged CFRPs

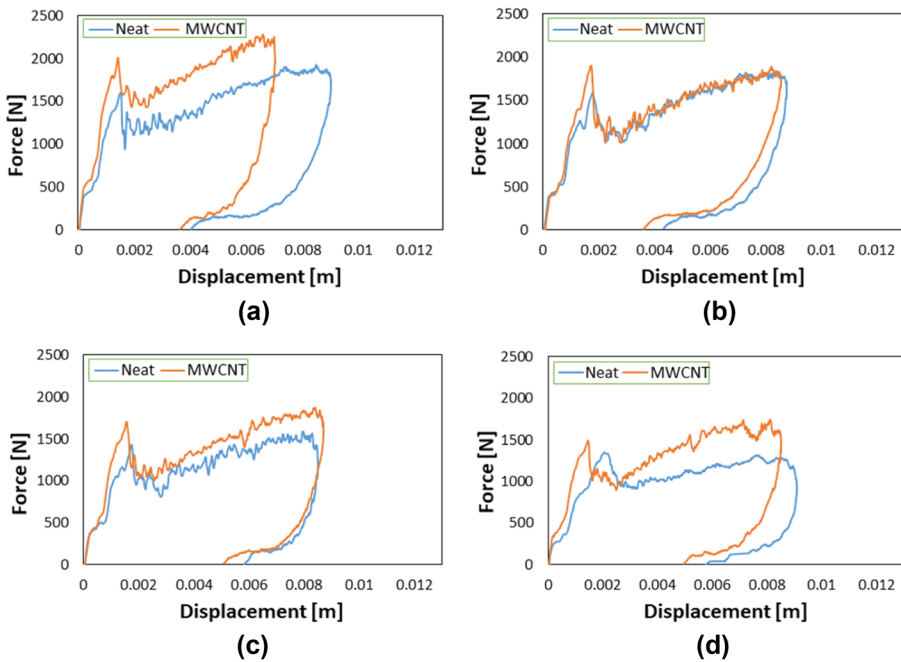


Fig. 15 Contact force–displacement variations at 10 J energy level for (a) Non-aged (b) 1 week, (c) 2 weeks, and (d) 3 weeks aged CFRPs

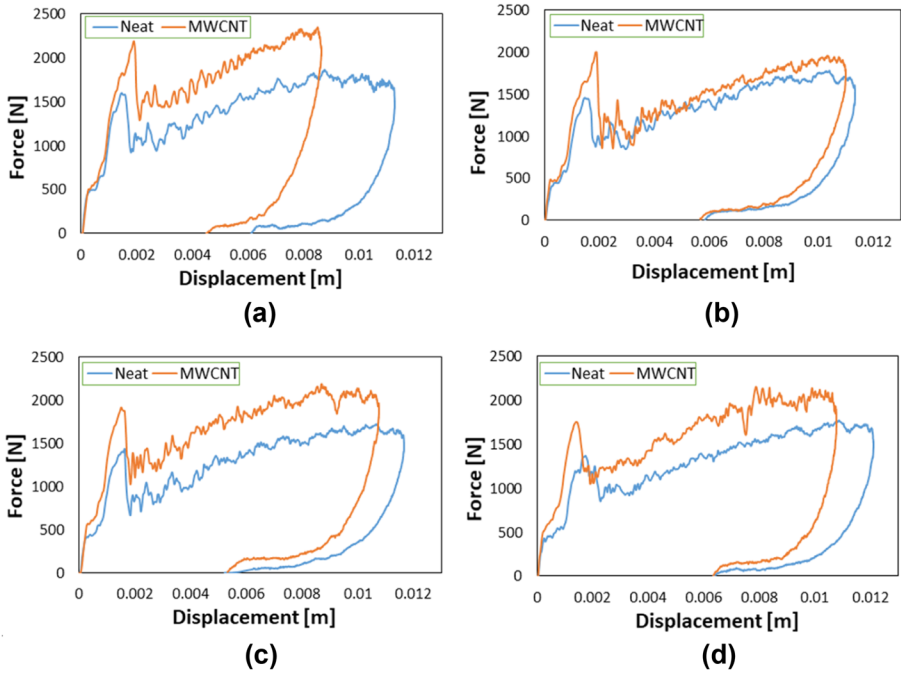


Fig. 16 Contact force–displacement variations at 15 J energy level for (a) Non-aged (b) 1 week, (c) 2 weeks, and (d) 3 weeks aged CFRPs

The aging process caused a loss in material stiffness. As a result, aged samples showed more elastic behavior against impacts. In the non-aged composite sample, which is fragile and rigid, the softening and deforming ability resulting from aging has changed the damage mechanism within the structure. A stress mismatch develops between the layers

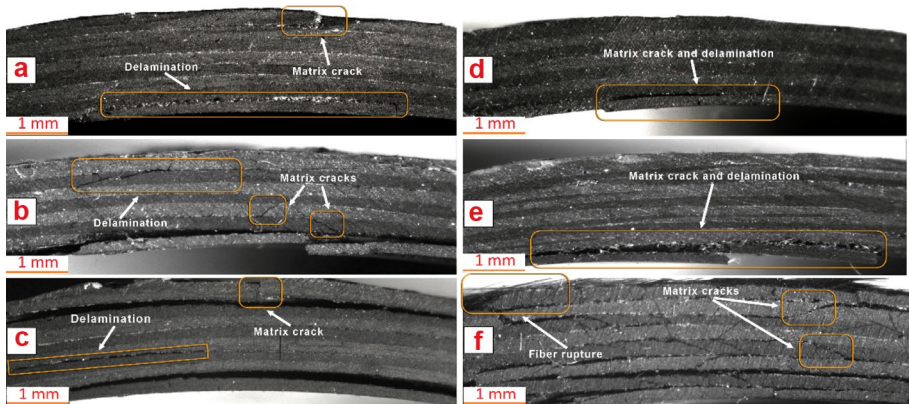


Fig. 17 Images of the cross-section of non-aged neat samples subjected to impact at (a) 5 J; (b) 10 J, (c) 15 J energy levels and non-aged MWCNT reinforced samples subjected to impact at (d) 5 J; (e) 10 J, (f) 15 J energy levels

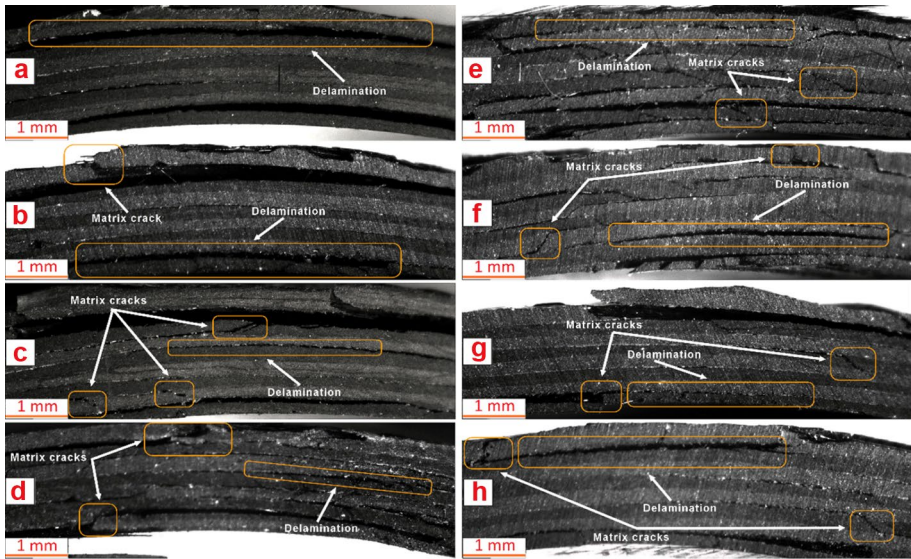


Fig. 18 Images of the cross-section of (a) non-aged; (b) 1 week, (c) 2 weeks, (d) 3 weeks aged neat and (e) non-aged; (f) 1 week, (g) 2 weeks, (h) 3 weeks aged MWCNT reinforced CFRPs damaged with the impact energy level of 15 J

because the layers have different stiffness. This mismatch causes delamination in the structure. Therefore, in aged samples, delaminations are observed rather than matrix cracking due to the effect of shear force. Thus, the impact strength of the material decreases as the aging period extends.

The most considerable deformations are seen in samples subjected to 15 J impact energy. Deformations occurred in almost every layer of these samples on a large scale. Damage images of samples with 15 J impact tests for various aging periods are presented in Fig. 18. It is seen that the deformation mechanism varies in the samples with nanoparticle added.

4 Conclusion

In this study, the effects of hydrothermal aging process on the mechanical strength and low speed impact behavior of neat and MWCNT reinforced carbon/epoxy composite pipes were investigated. The results obtained from the study are presented below.

- The highest tangential tensile strength value was obtained from MWCNT reinforced non-aged composite sample. The lowest tangential tensile strength was recorded in the neat sample aged for three weeks.
- The addition of nanoparticles strengthens matrix-fiber interface connections. For this reason, the tensile strength of nanoparticle added samples is higher than that of neat samples.
- The aging process causes a loss of strength in all samples. As a result of hydrothermal aging, the nanoparticles pass through the resin through diffusion, and porosity occurs in

the matrix. Then, the voids were formed by the nanoparticles coming out of the structure. For this reason, after three weeks of aging, tangential tensile strength loss was 17% in MWCNT reinforced sample and 13% in the neat sample.

- The addition of nanoparticle increases the impact resistance of the material as well as its tensile strength. The reason for this increase is that the nanoparticles strengthen the matrix-fiber interface connections and provide homogeneous diffusion of force with more surface areas in the material.
- It has been observed that nanoparticles ensure the homogeneous dissipation of the impact energy in the material. Thus, nanoparticles prevented large deformations in the local area within the structure. While damages in the neat composite pipes are mostly delaminations, matrix cracks have occurred in all layers in samples with nanoparticle addition. MWCNT added samples absorbed more impact energy and showed a more resistant feature against impacts.
- As a result of the aging process, rigidity of the samples decreased significantly. In samples that lost their rigidity, delaminations occurred instead of shear crack formation. Therefore, the first contact response to the impact in aged samples has decreased, but the contact time has increased. With the aging process, the impact resistance of the samples decreased.

Acknowledgements This study is a part of a Master Thesis that carried out by Safa AK at Necmettin Erbakan University, Institute of Science. Memduh KARA is the advisor of this thesis. This research didn't receive grants from any funding agency in public, commercial, or not-for-profit sectors.

Data Availability The data that support the findings of this study are available from the corresponding author upon reasonable request.

References

1. Gunoz, A., Kepir, Y., Kara, M.: Tensile Strength Alteration of GFRP Composite Pipes Under Seawater-Dominated Conditions. *J. Fail. Anal. Prev.* **20**(4), 1426–1430 (2020)
2. Kara, M., Kirici, M., Cagan, S.C.: Effects of the number of fatigue cycles on the hoop tensile strength of glass Fiber/epoxy composite pipes. *J. Fail. Anal. Prev.* **19**(4), 1181–1186 (2019)
3. Gemi, L., Kara, M., Avci, A.: Low velocity impact response of prestressed functionally graded hybrid pipes. *Compos. Part B Eng.* **106**, 154–163 (2016)
4. Demirci, M.T.: Low velocity impact and fracture characterization of SiO₂ nanoparticles filled basalt fiber reinforced composite tubes. *J. Compos. Mater.* **54**(23), 3415–3433 (2020)
5. Gunoz, A., Kepir, Y., Kara, M.: Effect of hydrothermal aging on the mechanical properties of nano-composite pipes. *Mater. Test.* **63**(3), 253–258 (2021)
6. Tarakçioğlu, N., Gemi, L., Yapici, A.: Fatigue failure behavior of glass/epoxy±55 filament wound pipes under internal pressure. *Compos. Sci. Technol.* **65**(3–4), 703–708 (2005)
7. Gemi, L., Kayıncı, M., Uludağ, M., Gemi, D.S., Şahin, Ö.S.: Experimental and statistical analysis of low velocity impact response of filament wound composite pipes. *Compos. Part B Eng.* **149**, 38–48 (2018)
8. Gemi, L., Şahin, Ö.S., Akdemir, A.: Experimental investigation of fatigue damage formation of hybrid pipes subjected to impact loading under internal pre-stress. *Compos. Part B Eng.* **119**, 196–205 (2017)
9. Şahin, Ö.S., Akdemir, A., Avci, A., Gemi, L.: Fatigue crack growth behavior of filament wound composite pipes in corrosive environment. *J. Reinf. Plast. Compos.* **28**(24), 2957–2970 (2009)
10. Eskizeybek, V., Ulus, H., Kaybal, H.B., Şahin, Ö.S., Avci, A.: Static and dynamic mechanical responses of CaCO₃ nanoparticle modified epoxy/carbon fiber nanocomposites. *Compos. Part B Eng.* **140**, 223–231 (2018)
11. Üstün, T., Ulus, H., Karabulut, S.E., Eskizeybek, V., Şahin, Ö.S., Avci, A., Demir, O.: Evaluating the effectiveness of nanofillers in filament wound carbon/epoxy multiscale composite pipes. *Compos. Part B Eng.* **96**, 1–6 (2016)

12. Taşyürek, M., Tarakçıoğlu, N.: Enhanced fatigue behavior under internal pressure of CNT reinforced filament wound cracked pipes. *Compos. Part B Eng.* **124**, 23–30 (2017)
13. Tehrani, M., Boroujeni, A.Y., Hartman, T.B., Haugh, T.P., Case, S.W., Al-Haik, M.S.: Mechanical characterization and impact damage assessment of a woven carbon fiber reinforced carbon nanotube–epoxy composite. *Compos. Sci. Technol.* **75**, 42–48 (2013)
14. Kara, M., Kırıcı, M., Tatar, A.C., Avci, A.: Impact behavior of carbon fiber/epoxy composite tubes reinforced with multi-walled carbon nanotubes at cryogenic environment. *Compos. Part B Eng.* **145**, 145–154 (2018)
15. Laurenzi, S., Pastore, R., Giannini, G., Marchetti, M.: Experimental study of impact resistance in multi-walled carbon nanotube reinforced epoxy. *Compos. Struct.* **99**, 62–68 (2013)
16. Demirci, I., Avci, A., Demirci, M.T.: Investigation of nano-hybridization effects on low velocity impact behaviors of basalt fiber reinforced composites. *J. Compos. Mater.* 0021998320949640 (2020)
17. Fan, X., Lee, S., Han, Q.: Experimental investigations and model study of moisture behaviors in polymeric materials. *Microelectron. Reliab.* **49**(8), 861–871 (2009)
18. Yang, B., Zhang, J., Zhou, L., Lu, M., Liang, W., Wang, Z.: Effect of fiber surface modification on water absorption and hydrothermal aging behaviors of GF/pCBT composites. *Compos. Part B Eng.* **82**, 84–91 (2015)
19. Lu, Z., Xian, G., Li, H.: Effects of exposure to elevated temperatures and subsequent immersion in water or alkaline solution on the mechanical properties of pultruded BFRP plates. *Compos. Part B Eng.* **77**, 421–430 (2015)
20. Nayak, R.K., Mahato, K.K., Ray, B.C.: Water absorption behavior, mechanical and thermal properties of nano TiO₂ enhanced glass fiber reinforced polymer composites. *Compos. Part A Appl. Sci. Manuf.* **90**, 736–747 (2016)
21. Alessi, S., Pitarresi, G., Spadaro, G.: Effect of hydrothermal ageing on the thermal and delamination fracture behaviour of CFRP composites. *Compos. Part B Eng.* **67**, 145–153 (2014)
22. Barbosa, A.P.C., Fulco, A.P.P., Guerra, E.S., Arakaki, F.K., Tosatto, M., Costa, M.C.B., Melo, J.D.D.: Accelerated aging effects on carbon fiber/epoxy composites. *Compos. Part B Eng.* **110**, 298–306 (2017)
23. Nor, A.F.M., Sultan, M.T.H., Jawaid, M., Azmi, A.M.R., Shah, A.U.M.: Analysing impact properties of CNT filled bamboo/glass hybrid nanocomposites through drop-weight impact testing, UWPI and compression-after-impact behaviour. *Compos. Part B Eng.* **168**, 166–174 (2019)
24. El. Moumen, A., Tarfaoui, M., Lafdi, K., Benyahia, H.: Dynamic properties of carbon nanotubes reinforced carbon fibers/epoxy textile composites under low velocity impact. *Compos. Part B Eng.* **125**, 1–8 (2017)
25. Kara, M., Uyaner, M., Avci, A., Akdemir, A.: Effect of non-penetrating impact damages of pre-stressed GRP tubes at low velocities on the burst strength. *Compos. Part B Eng.* **60**, 507–514 (2014)
26. Uyaner, M., Kara, M., Şahin, A.: Fatigue behavior of filament wound E-glass/epoxy composite tubes damaged by low velocity impact. *Compos. Part B Eng.* **61**, 358–364 (2014)
27. Kara, M., Kırıcı, M.: Effects of the number of fatigue cycles on the impact behavior of glass fiber/epoxy composite tubes. *Compos. Part B Eng.* **123**, 55–63 (2017)
28. Taraghi, I., Fereidoon, A.: Non-destructive evaluation of damage modes in nanocomposite foam-core sandwich panel subjected to low-velocity impact. *Compos. Part B Eng.* **103**, 51–59 (2016)
29. Ranjbar, M., Feli, S.: Mechanical and low-velocity impact properties of epoxy-composite beams reinforced by MWCNTs. *J. Compos. Mater.* **53**(5), 693–705 (2019)
30. Benyahia, H., Tarfaoui, M., El. Moumen, A., Ouinas, D.: Prediction of notched strength for cylindrical composites pipes under tensile loading conditions. *Compos. Part B Eng.* **150**, 104–114 (2018)
31. Demirci, M.T., Tarakçıoğlu, N., Avci, A., Akdemir, A., Demirci, I.: Fracture toughness (Mode I) characterization of SiO₂ nanoparticle filled basalt/epoxy filament wound composite ring with split-disk test method. *Compos. Part B Eng.* **119**, 114–124 (2017)
32. Shabani, P., Taheri-Behrooz, F., Maleki, S., Hasheminasab, M.: Life prediction of a notched composite ring using progressive fatigue damage models. *Compos. Part B Eng.* **165**, 754–763 (2019)
33. Sepetcioğlu, H., Gunoz, A., Kara, M.: Effect of hydrothermal ageing on the mechanical behaviour of graphene nanoplatelets reinforced basalt fibre epoxy composite pipes. *Polym. Compos.* 0967391121992939 (2021)
34. Zhou, Y., Pervin, F., Lewis, L., Jeelani, S.: Experimental study on the thermal and mechanical properties of multi-walled carbon nanotube-reinforced epoxy. *Mater. Sci. Eng. A* **452**, 657–664 (2007)
35. Zhou, Y., Jeelani, M., Jeelani, S.: Development of photo micro-graph method to characterize dispersion of CNT in epoxy. *Mater. Sci. Eng. A* **506**(1–2), 39–44 (2009)
36. Zhou, Y., Pervin, F., Lewis, L., Jeelani, S.: Fabrication and characterization of carbon/epoxy composites mixed with multi-walled carbon nanotubes. *Mater. Sci. Eng. A* **475**(1–2), 157–165 (2008)

37. ASTM: ASTM D2290: Standard test method for apparent hoop tensile strength of plastic or reinforced plastic pipe. In. ASTM International, West Conshohocken. (2012)
38. Ak, S.: The effect of hydrothermal aging on the mechanical properties of carbon fiber-epoxy composite pipes with carbon nanotube and boron nitride nano particles. Master Thesis (2019), Necmettin Erbakan University, Institute of Science, Konya (Turkish)
39. Karabulut, S.E.: The effect of carbon nanotube and boron nitride nanoparticles addition on dynamic behaviour of filament wound carbon fiber/epoxy pipes. PhD Dissertation (2017), Selçuk University, Insitute of Science, Konya (Turkish)
40. Uyaner, M.: Test to Graph. In. Mendeley Data, V2. (2020)
41. El Moumen, A., Tarfaoui, M., Lafdi, K.: Mechanical characterization of carbon nanotubes based polymer composites using indentation tests. *Compos. Part B Eng.* **114**, 1–7 (2017)
42. Ma, H.-L., Jia, Z., Lau, K.-T., Leng, J., Hui, D.: Impact properties of glass fiber/epoxy composites at cryogenic environment. *Compos. Part B Eng.* **92**, 210–217 (2016)
43. International, A.: ASTM Standard D7136/D7136M-15: Standard Test Method for Measuring the Damage Resistance of a Fiber-Reinforced Polymer Matrix Composite to a Drop-Weight Impact Event. In. ASTM International West Conshohocken, PA. (2015)

Publisher's Note Springer Nature remains neutral with regard to jurisdictional claims in published maps and institutional affiliations.